EPJ manuscript No.
(will be inserted by the editor)

arXiv:cond-mat/0309322v2 [cond-mat.soft] 5 Nov 2003

Indirect interactions of membrane-adsorbed cylinders

Thomas R. Weikl

Max-Planck-Institut für Kolloid- und Grenzflächenforschung, 14424 Potsdam, Germany

Abstract. Biological and biomimetic membranes often contain aggregates of embedded or adsorbed macromolecules. In this article, the indirect interactions of cylindrical objects adhering to a planar membrane are considered theoretically. The adhesion of the cylinders causes a local perturbation of the equilibrium membrane shape, which leads to membrane-mediated interactions. For a planar membrane under lateral tension, the interaction is repulsive for a pair of cylinders adhering to the same side of the membrane, and attractive for cylinders adhering at opposite membrane sides. For a membrane in an external harmonic potential, the interaction of adsorbed cylinders is always attractive and increases if forces perpendicular to the membrane act on the cylinders.

PACS. 87.16.Dg Membranes, bilayers, and vesicles – 34.20-b Interatomic and intermolecular potentials and forces, potential energy surfaces for collisions

1 Introduction

Biological membranes consist of a multi-component lipid bilayer with a variety of embedded or adsorbed macromolecules such as proteins [1,2]. In recent years, experiments revealed a complex lateral architecture of these membranes which contain domains or 'rafts' of different molecular composition. The domains often serve important biological functions in signaling [3], budding [4], or cell adhesion [5,6].

Lateral phase separation and domain formation has also been observed for biomimetic membranes, which are composed of only a few different molecules. In principal, the phase separation may either be caused (i) by a demixing of the lipid bilayer [7,8], or (ii) by the aggregation of embedded or adsorbed macromolecules [9,10]. To understand the latter, membrane-mediated interactions between macromolecules have been studied intensively. They can be divided into static and dynamic interactions. *Dynamic*, or Casimir-like, interactions arise from the suppression of membrane shape fluctuations by embedded macromolecules such as rigid inclusions [11,12,13,14,15, 16,17] or specific receptors or stickers [18,19]. *Static* interactions are due to a perturbation of the equilibrium bilayer structure or equilibrium membrane shape by the embedded or adsorbed macromolecules. Examples for such macromolecules are trans-membrane proteins [20,21,22, 23,24] and adsorbed molecules [25] causing a perturbation of the equilibrium membrane thickness, as well as conical or anisotropic inclusions [11,26,27,28,29,15,30] and membrane-anchored polymers [31,32] which cause a perturbation of the equilibrium membrane curvature.

In this article, the static interactions of parallel cylindrical objects adhering to a planar membrane are considered. A single such cylinder has been recently studied in Ref. [33]. The cylinders are characterized by their radius R and a favorable adhesion energy per area U which is balanced in equilibrium by the elastic energy of the membrane shape deformation. Examples for such objects are cylindrical viruses or coated latex cylinders similar to the beads considered in Ref. [10]. The membrane shape around an adsorbed cylinder is similar to the shape around an elongated wedge-shaped inclusion characterized by its diameter D and angle α. However, the pair interaction energies are different since the contact area of parallel adsorbed cylinders depends on the distance L between the cylinders, while the diameter D and angle α of wedge-shaped inclusions are constant.

2 General model and geometry

In the absence of adhering objects, the membrane considered here is planar and constrained into the x-y plane either by a lateral tension σ (section 3) or by a harmonic potential (section 4). The adhering cylinders are characterized by their radius R and adhesion energy U per area. The cylinders are assumed to be parallel and to be much longer than their distance L. The membrane profile then is approximated by the one-dimensional function $h(x)$ measuring the deviation out of the x-y plane. Here, x is the cartesian coordinate perpendicular to the cylinder axes. The membrane bending energy per area is given by $\frac{1}{2}\kappa h''(x)^2$ where κ is the bending rigidity and $h''(x)$ is the total membrane curvature.

In order to determine the equilibrium membrane energy, we first determine the shape and energy of the membrane as a function of the contact area with the cylinder(s). For a single cylinder with axis located at $x = 0$,

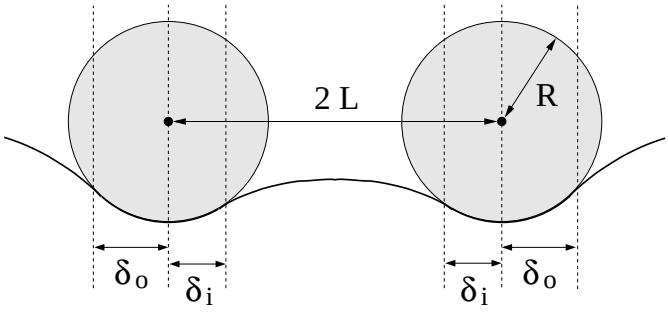

Fig. 1. Sketch of a membrane with two parallel cylinders adhering at the same side.

the contact area is given by $|x| < \delta_o$. For a pair of cylinders with axes located at $x = \pm L$, the contact areas are given by $L - \delta_\iota < |x| < L + \delta_o$ (see Fig. 1). In equilibrium, the system is 'free' to choose its contact area. Therefore, we finally minimize the free energy with respect to the contact parameters δ_o, δ_ι and the deviation h_o of the cylinders out of the x-y plane. In the case of a single cylinder, the contact parameter δ_o divides the membrane into the contact region and the two 'outer' membrane regions with $|x| > \delta_o$. In the case of two cylinders, we have two contact regions, an 'inner' membrane region with $|x| < L - \delta_\iota$ between the cylinders, and two 'outer' membrane regions with $|x| > L + \delta_o$.

3 Membrane under lateral tension

In the presence of a lateral tension σ, the elastic energy of the membrane can be written as

$$G = \int \left(\frac{\kappa}{2} h''(x)^2 + \frac{\sigma}{2} h'(x)^2 \right) dx \qquad (1)$$

where $h(x)$ is the membrane profile perpendicular to the adhering cylinder(s), and κ is the bending rigidity. Here, $\frac{1}{2}h'(x)^2$ is the local area increase with respect to the x-y plane. The membrane profile $h(x)$ outside of the contact region with the cylinder(s) has to fulfill the Euler–Lagrange equation

$$h''''(x) - \xi^2 h''(x) = 0 \qquad (2)$$

associated with eq. (1). Here, $\xi = \sqrt{\sigma/\kappa}$ is a characteristic reciprocal length. A general solution of the Euler–Lagrange equation (2) is given by

$$h(x) = C_1 + C_2 x + C_3 \exp(-\xi x) + C_4 \exp(\xi x) \qquad (3)$$

The tension σ is assumed to be constant here. Strictly speaking, this assumption presupposes a membrane area reservoir, since the overall area increase of the membrane with respect to the reference plane then depends on the distance of the cylinders.

3.1 Single cylinder

We first consider a single cylinder adhering to the membrane in the absence of an external force. The center of the cylinder is located at $x = 0$, and the membrane adheres to the cylinder for $-\delta_o < x < \delta_o$. The membrane segment in contact with the cylinder has the circular profile

$$h(x) = h_o - \sqrt{R^2 - x^2} + R \simeq h_o + \frac{x^2}{2R} \qquad (4)$$

for $\delta_o \ll R$, where R is the cylinder radius. For $|x| > \delta_o$, the profile of the membrane has the form

$$h(x) = A + B \exp(-\xi |x|) \qquad (5)$$

For $A = 0$, the profile fulfills the boundary condition $h(x) \to 0$ for $|x| \to \infty$. The constants B in eq. (5) and h_o in eq. (4) can be determined from the conditions of continuous profile $h(x)$ and slope $h'(x)$ at $x = \delta_o$. From the latter condition, we obtain $B = -\delta_o/(\xi R)$ to first order in δ_o. The energy G_z of the adhering membrane with profile (4) is the sum of the elastic energy (1) and the adhesion energy. To second order in δ_o, the energy of the adhering membrane is given by

$$G_z = 2\delta_o \left(\frac{\kappa}{2R^2} + U \right) \qquad (6)$$

where U is the adhesion energy per area. The energy of the 'outer' membrane segments with $|x| > \delta_o$ is

$$G_o = \frac{\sqrt{\sigma\kappa}\,\delta_o^2}{R^2} \qquad (7)$$

From the equilibrium condition $\partial G/\partial \delta_o = 0$ with $G = G_z + G_o$, we obtain

$$\delta_o = -\frac{\kappa + 2R^2 U}{2\sqrt{\sigma\kappa}} \qquad (8)$$

The cylinder is bound to the membrane for $\delta_o > 0$, i.e. for $U < -\kappa/(2R^2)$. Thus, to obtain a bound state, the adhesion energy U has to compensate at least the bending energy $\kappa/(2R^2)$ of the membrane with curvature $1/R$ at the cylinder. Inserting (8) into the total membrane energy $G = G_z + G_o$ leads to

$$G = -\frac{(\kappa + 2R^2 U)^2}{4\sqrt{\sigma\kappa} R^2} \qquad (9)$$

The profile of a membrane with a single adsorbed cylinder is shown in Fig. 2.

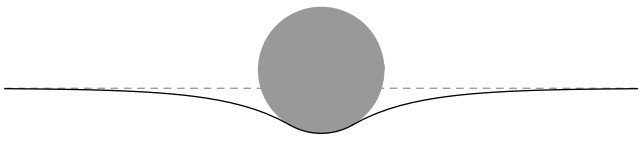

Fig. 2. Minimum energy profile for a single cylinder adhering to a membrane under a lateral tension σ. The rescaled adhesion energy is $\tilde{U} = 2UR^2/\kappa = -2$, and the inverse characteristic length $\xi = \sqrt{\sigma/\kappa}$ has the value $\xi = 1/R$ where R is the cylinder radius.

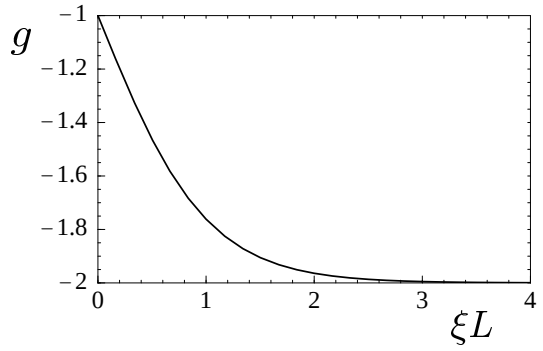

Fig. 3. Dimensionless interaction energy $g(L) = -(1 + \tanh(\xi L))$ of two cylinders adhering to the *same* side of a membrane under lateral tension (see eq. (13)). Here, ξL is the rescaled distance of the cylinders.

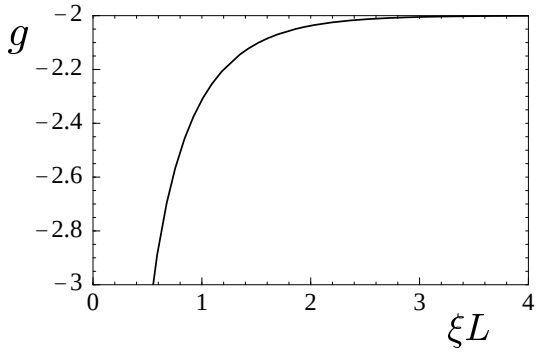

Fig. 4. Dimensionless interaction energy $g(L) = -(1 + \coth(\xi L)$ of two cylinders adhering to *opposite* sides of a membrane under lateral tension (see eq. (21)). Here, ξL is the rescaled distance of the cylinders.

3.2 Two cylinders at same membrane side

We now consider a membrane in contact with two parallel cylinders with centers located at $x = \pm L$. In this section, the cylinders adhere at the same side of the membrane. We assume first that the membrane is bound to the cylinders for $L - \delta_\iota < |x| < L + \delta_o$, and later determine the contact points $L-\delta_\iota$ and $L+\delta_o$ from a minimization of the energy. A general solution for the shape of the 'inner' membrane segment with $|x| < L-\delta_\iota$ obeying the symmetry condition $h(x) = h(-x)$ is

$$h(x) = C + D\cosh(\xi x) \tag{10}$$

From the condition of continuous slope $h'(x)$ at $x = L-\delta_\iota$, we obtain $D = -\delta_\iota/(\xi R \sinh(\xi L))$ to first order in δ_ι. To second order in δ_ι, the energy of the 'inner' membrane segment with $-(L - \delta_\iota) < x < L - \delta_\iota$ is

$$G_\iota = \frac{\sqrt{\sigma\kappa}\delta_\iota^2}{\tanh(\xi L)R^2} \tag{11}$$

The total energy of the membrane is $G = G_\iota + G_o + G_z$ with G_o given in eq. (7) and $G_z = 2(\delta_\iota + \delta_o)(U + \kappa/(2R^2))$ as in the previous section. The contact parameters δ_ι and δ_o follow from the equilibrium conditions $\partial G/\partial\delta_\iota = 0$ and $\partial G/\partial\delta_o = 0$. We obtain

$$\delta_\iota = -\frac{(\kappa + 2R^2U)\tanh(\xi L)}{2\sqrt{\sigma\kappa}} \tag{12}$$

and δ_o as in eq. (8), and the interaction energy

$$\boxed{G(L) = -\frac{(\kappa + 2R^2U)^2(1 + \tanh(\xi L))}{4\sqrt{\sigma\kappa}R^2}} \tag{13}$$

The interaction energy is repulsive, attaining its minimum $G = -(\kappa + 2R^2U)^2/(2\sqrt{\sigma\kappa}R^2)$ for $L \to \infty$. The dimensionless interaction energy $g(L) = 4\sqrt{\sigma\kappa}R^2G(L)/(\kappa + 2R^2U)^2$ is shown in Fig. 3.

3.3 Two cylinders at opposite membrane sides

In this section, we consider two cylinders adhering at opposite sides of the membrane. We assume that the 'right' cylinder with axis at $x = L$ is on top of the membrane, and the 'left' cylinder at $x = -L$ below the membrane. The membrane segment with $L - \delta_\iota < x < L + \delta_o$ adhering to the right cylinder then has the profile

$$h(x) = h_o + \frac{(x - L)^2}{2R} \tag{14}$$

for $\delta_\iota \ll R$ and $\delta_o \ll R$. For symmetry reasons we now have $h(-x) = -h(x)$. Therefore, the general solution for the profile of the 'inner' membrane segment with $|x| < L - \delta_\iota$ is

$$h(x) = Cx + D\sinh(\xi x) \tag{15}$$

From the boundary conditions of continuous profile h and slope h' at $x = L - \delta_\iota$, we obtain

$$C = \frac{\xi R h_o \cosh(\xi L) + \delta_\iota \sinh(\xi L)}{R(\xi L\cosh(\xi L) - \sinh(\xi L))} \tag{16}$$

$$D = \frac{L\delta_\iota + Rh_o}{R(\sinh(\xi L) - \xi L\cosh(\xi L))} \tag{17}$$

to first order in h_o and δ_ι. To second order in h_o and δ_ι, the energy of the 'inner' membrane segment with $|x| < L - \delta_\iota$ is

$$G_\iota = \frac{\sigma[\xi R^2 h_o^2\cosh(\xi L) + \delta_\iota(L\delta_\iota + 2Rh_o)\sinh(\xi L)]}{R^2[\xi L\cosh(\xi L) - \sinh(\xi L)]} \tag{18}$$

As in the previous sections, the energy G_o of the two 'outer' segments is given by eq. (7), and the energy of the two adhering membrane segments is $G_z = 2(\delta_\iota + \delta_o)(U + \kappa/(2R^2))$. Minimizing the total membrane energy $G = G_z + G_\iota + G_o$ with respect to δ_ι, δ_o, and h_o leads to

$$\delta_\iota = -\frac{(\kappa + 2R^2U)\coth(\xi L)}{2\sqrt{\sigma\kappa}} \tag{19}$$

$$h_o = \frac{\kappa + 2R^2U}{2\sigma R} \tag{20}$$

and δ_o as in eq. (8), and the attractive interaction energy

$$\boxed{G(L) = -\frac{(\kappa + 2R^2U)^2(1+\coth(\xi L))}{4\sqrt{\sigma\kappa}R^2}} \qquad (21)$$

The dimensionless energy $g(L) = 4\sqrt{\sigma\kappa}R^2G(L)/(\kappa+2R^2U)^2$ is shown in Fig. 4.

4 Harmonic potential

In this section, we assume that the membrane is bound in an external potential, induced, e.g., by a substrate supporting the membrane, or an elastic mesh coupled to the membrane. In harmonic approximation, the elastic energy of the membrane then can be written as

$$G = \int \left(\frac{\kappa}{2}h''(x)^2 + \frac{m}{2}h(x)^2\right) dx \qquad (22)$$

where m is the harmonic potential strength, and $h(x)$ is the membrane profile perpendicular to the cylinders. We now neglect the lateral tension σ. This is justified as long as $\eta \equiv (m/(4\kappa))^{1/4}$, the characteristic inverse length for a membrane in a harmonic potential, is much larger than $\xi = \sqrt{\sigma/\kappa}$. The Ginzburg-Landau equation reads

$$h''''(x) + 4\eta^4 h(x) = 0 \qquad (23)$$

A general solution of this differential equation is

$$h(x) = C_1\exp(\eta x)\cos(\eta x) + C_2\exp(\eta x)\sin(\eta x) + C_3\exp(-\eta x)\cos(\eta x) + C_4\exp(-\eta x)\sin(\eta x) \qquad (24)$$

4.1 Single cylinder

The profile of the membrane segment adhering to the cylinder for $|x| \le \delta_o$ is again given by eq. (4). To second order in δ_o and h_o, the energy G_z of this membrane segment is the same as in eq. (6). The harmonic potential contributes a third-order term to G_z which is neglected here.

For $|x| > \delta_o$, the membrane has the form

$$h(x) = A\exp(-\eta|x|)\cos(\eta|x|) + B\exp(-\eta|x|)\sin(\eta|x|) \qquad (25)$$

which obeys the boundary condition $h(x) \to 0$ for $|x| \to \infty$. The coefficients A and B follow again from the boundary conditions of continuous profile $h(x)$ and slope $h'(x)$ at $x = \pm\delta_o$. To leading order in δ_o and h_o, these coefficients are given by $A = h_o + \delta_o/(\eta R)$ and $B = h_o$. To second order in δ_o and h_o, the energy of the 'outer' membrane segments with $|x| > \delta_o$ reads

$$G_o = \frac{2\eta\kappa}{R^2}(\delta_o^2 + 2\eta R\delta_o h_o + 2\eta^2R^2h_o^2) \qquad (26)$$

The contact point δ_o and height h_o follow from the equilibrium conditions $\partial G/\partial h_o = 0$ and $\partial G/\partial\delta_o = 0$ where

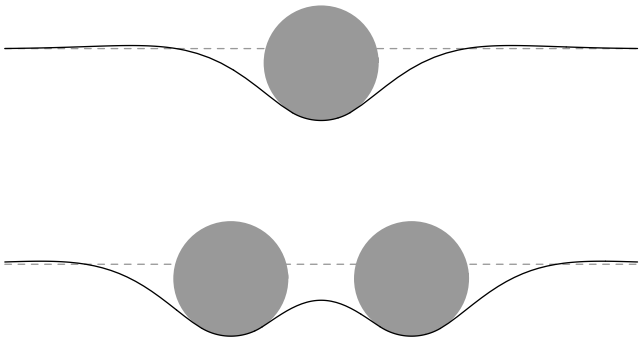

Fig. 5. Minimum energy profiles for (top) a single adsorbed cylinder and (bottom) two cylinders adhering at the same side of a membrane in a harmonic potential with strength m. The rescaled adhesion energy is $\tilde{U} = 2UR^2/\kappa = -2$, and the inverse characteristic length $\eta = (m/(4\kappa))^{1/4}$ has the value $\eta = 1/R$ where R is the cylinder radius.

$G = G_z + G_o$ is the total membrane energy. We obtain

$$\delta_o = -\frac{\kappa + 2R^2U}{2\eta\kappa} \qquad (27)$$

$$h_o = \frac{\kappa + 2R^2U}{4\eta^2\kappa R} \qquad (28)$$

and the energy

$$G = -\frac{(\kappa + 2R^2U)^2}{4\eta\kappa R^2} \qquad (29)$$

If an external force F is acting on the cylinder perpendicular to the membrane plane, the total energy is $G = G_z + G_o + Fh_o$. Minimizing G now leads to

$$\delta_o = \frac{FR - 2\eta(\kappa + 2R^2U)}{4\eta^2\kappa} \qquad (30)$$

$$h_o = \frac{-FR + \eta(\kappa + 2R^2U)}{4\eta^3\kappa R} \qquad (31)$$

The cylinder unbinds from the membrane if the contact parameter δ_o, and thus the contact area, equals zero. The threshold force leading to unbinding is

$$F_t = 2\eta(\kappa + 2R^2U)/R \qquad (32)$$

4.2 Two cylinders at same membrane side

Let us now consider a membrane with two cylinders adhering at the same side of the membrane. For symmetry reasons, the shape of the 'inner' membrane segment with $|x| < L - \delta_\iota$ is given by

$$h(x) = C\sinh(\eta x)\sin(hx) + D\cosh(\eta x)\cos(\eta x) \qquad (33)$$

The coefficients are again obtained from the boundary conditions of continuous profile $h(x)$ and slope $h'(x)$ at

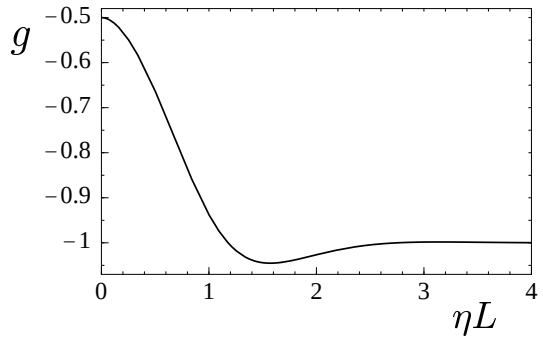

Fig. 6. Dimensionless interaction energy $g(L) = -\exp(2\eta L)/(\exp(2\eta L)+\cos(2\eta L)+\sin(2\eta L))$ of two cylinders adhering to the *same* side of a membrane in a harmonic potential (see eq. (40)).

$x = \pm(L-\delta_\iota)$. To first order in δ_ι and h_o they read

$$C = \frac{2}{\eta R \Phi_1}\big\{[\eta R h_o \sin(\eta L) - \delta_\iota \cos(\eta L)]\cosh(\eta L) - \eta R h_o \cos(\eta L)\sinh(\eta L)\big\} \quad (34)$$

$$D = \frac{2}{\eta R \Phi_1}\big\{[\eta R h_o \cos(\eta L) + \delta_\iota \sin(\eta L)]\sinh(\eta L) + \eta R h_o \cosh(\eta L)\sin(\eta L)\big\} \quad (35)$$

with $\Phi_1 = \sin(2\eta L)+\sinh(2\eta L)$. To second order in δ_ι and h_o, the energy of the inner membrane segment is given by

$$G_\iota = \frac{2\eta\kappa}{R^2\Phi_1}\Big\{(\delta_\iota^2 - 2\eta^2R^2h_o^2)\cos(2\eta L) + (\delta_\iota^2 + 2\eta^2R^2h_o^2)\times \times\cosh(2\eta L) + 2\eta R\delta_\iota h_o[\sinh(2\eta L) - \sin(2\eta L)]\Big\} \quad (36)$$

Minimizing the total membrane energy $G = G_\iota + G_o + G_z$ with $G_z = 2(\delta_\iota+\delta_o)(U+\kappa/(2R^2))$ and G_o as given in eq. (26) with respect to δ_ι, δ_o, and h_o leads to

$$\delta_\iota = -\frac{(\kappa+2R^2U)(\exp(2\eta L)-\cos(2\eta L))}{2\eta\kappa(\exp(2\eta L)+\cos(2\eta L)+\sin(2\eta L))} \quad (37)$$

$$\delta_o = -\frac{(\kappa+2R^2U)(\exp(2\eta L)+\cos(2\eta L))}{2\eta\kappa(\exp(2\eta L)+\cos(2\eta L)+\sin(2\eta L))} \quad (38)$$

$$h_o = \frac{(\kappa+2R^2U)(\exp(2\eta L)+\cos(2\eta L)-\sin(2\eta L))}{4\eta^2\kappa R(\exp(2\eta L)+\cos(2\eta L)+\sin(2\eta L))} \quad (39)$$

and the interaction energy

$$\boxed{G(L) = -\frac{(\kappa+2R^2U)^2\exp(2\eta L)}{2\eta\kappa R^2[\exp(2\eta L)+\cos(2\eta L)+\sin(2\eta L)]}} \quad (40)$$

The dimensionless energy $g(L) = 2\eta\kappa R^2 G(L)/(\kappa+2R^2U)^2$ is shown in Fig. 6. The global minimum of the interaction energy is at $L_{\min} = \pi/(2\eta)$ (see also Fig. 5).

4.3 Two cylinders at opposite membrane sides

In this section, we consider two cylinders adhering at opposite sides of a membrane in a harmonic potential. As in section 3.3, we assume that the 'right' cylinder with axis at $x = L$ is above the membrane, and the left cylinder at $x = -L$ is below the membrane. The profile of the membrane has the symmetry $h(-x) = -h(x)$. Therefore, the profile of the 'inner' membrane segment with $|x| < L - \delta_\iota$ has the general form

$$h(x) = C\cosh(\eta x)\sin[hx] + D\sinh(\eta x)\cos(\eta x) \quad (41)$$

From the conditions of continuous profile $h(x)$ and slope $h'(x)$ at $x = \pm(L-\delta_\iota)$, we obtain to first order in δ_ι and h_o:

$$C = \frac{2}{\eta R\Phi_2}\big\{\eta R h_o[(\cosh(\eta L)\cos(\eta L) - \sinh(\eta L)\sin(\eta L)] + \delta_\iota\sinh(\eta L)\cos(\eta L)\big\} \quad (42)$$

$$D = -\frac{2}{\eta R\Phi_2}\big\{\eta R h_o[(\cosh(\eta L)\cos(\eta L) + \sinh(\eta L)\sin(\eta L)] + \delta_\iota\cosh(\eta L)\sin(\eta L)\big\} \quad (43)$$

with $\Phi_2 = \sin(2\eta L) - \sinh(2\eta L)$. To second order in δ_ι and h_o, the energy of the inner membrane segment is given by

$$G_\iota = \frac{2\eta\kappa}{R^2\Phi_2}\Big\{(\delta_\iota^2 - 2\eta^2R^2h_o^2)\cos(2\eta L) - (\delta_\iota^2 + 2\eta^2R^2h_o^2)\times \times\cosh(2\eta L) - 2\eta R\delta_\iota h_o[\sinh(2\eta L) + \sin(2\eta L)]\Big\} \quad (44)$$

Minimizing the total membrane energy $G = G_\iota + G_o + G_z$, with $G_z = 2(\delta_\iota+\delta_o)(U+\kappa/(2R^2))$ and G_o given in eq. (26) leads to

$$\delta_\iota = -\frac{(\kappa+2R^2U)(\exp(2\eta L)+\cos(2\eta L))}{2\eta\kappa(\exp(2\eta L)-\cos(2\eta L)-\sin(2\eta L))} \quad (45)$$

$$\delta_o = -\frac{(\kappa+2R^2U)(\exp(2\eta L)-\cos(2\eta L))}{2\eta\kappa(\exp(2\eta L)-\cos(2\eta L)-\sin(2\eta L))} \quad (46)$$

$$h_o = \frac{(\kappa+2R^2U)(\exp(2\eta L)-\cos(2\eta L)+\sin(2\eta L))}{4\eta^2\kappa R(\exp(2\eta L)-\cos(2\eta L)-\sin(2\eta L))} \quad (47)$$

and the interaction energy

$$\boxed{G(L) = -\frac{(\kappa+2R^2U)^2\exp(2\eta L)}{2\eta\kappa R^2[\exp(2\eta L)-\cos(2\eta L)-\sin(2\eta L)]}} \quad (48)$$

The dimensionless interaction energy $g(L) = 2\eta\kappa R^2 G(L)/(\kappa+2R^2U)^2$ is shown in Fig. 7.

4.4 External force

In the presence of an external force F acting on the cylinders perpendicular to membrane plane, the total energy for given contact parameters δ_ι and δ_o and given h_o is $G = G_z(\delta_\iota,\delta_o) + G_\iota(\delta_\iota,h_o) + G_o(\delta_o,h_o) + 2Fh_o$. Minimizing G with respect to δ_o, δ_ι, and h_o leads to

$$G(L) = -\frac{(\kappa+2R^2U)^2}{2\eta\kappa R^2\Phi_3}\Big\{e^{2\eta L} + \tilde{F}\big[e^{2\eta L} + \cos(2\eta L) - \sin(2\eta L)\big] + \tilde{F}^2[\cosh(2\eta L) + \cos(2\eta L)]\Big\} \quad (49)$$

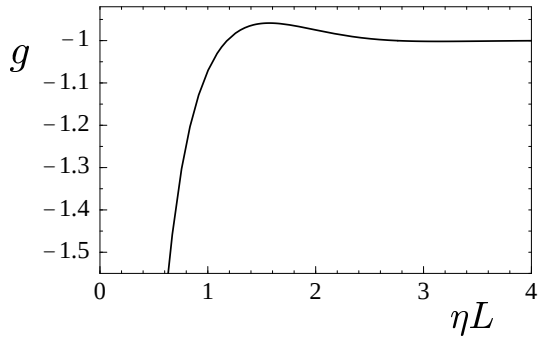

Fig. 7. Dimensionless interaction energy $g(L) = -\exp(2\eta L)/(\exp(2\eta L) - \cos(2\eta L) - \sin(2\eta L))$ of two cylinders adhering to *opposite* sides of a membrane in a harmonic potential (see eq. (48)).

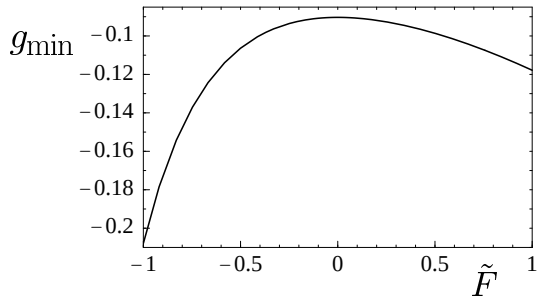

Fig. 8. Dimensionless binding energy $g_{\min}$ as a function of the rescaled force $\tilde{F}$ for two cylinders adhering at the same side of a membrane in a harmonic potential. The absolute value of the binding energy $g_{\min}$ *increases* under an applied force $\tilde{F}$, irrespective of the sign of $\tilde{F}$.

with $\Phi_3 = \exp(2\eta L)+\cos(2\eta L)+\sin(2\eta L)$ and the rescaled force $\tilde{F} = -FR/[\eta(\kappa + 2R^2U)]$.

Fig. 8 shows the dimensionless binding energy of the cylinders $g_{\min} = (G(L_{\min})-G(\infty))\times(2\eta\kappa R^2)/(\kappa+2R^2U)^2$ as a function of the rescaled force $\tilde{F}$. Here, $L_{\min}$ is the cylinder separation at which the interaction energy $G(L)$ has its minimum. The binding energy of the two cylinders increases irrespective of the sign of the force, i.e. both for perpendicular forces pulling on the cylinders, and for forces pushing the cylinders into the membrane.

5 Discussion

We have considered the indirect interactions of parallel cylindrical objects adhering to a planar membrane. The interactions arise from the perturbations of the equilibrium membrane shape caused by the cylinders. The cylinders are assumed to be much longer than their distance L, and the membrane profile is approximated by a one--dimensional function $h(x)$. Here, x is a cartesian coordinate perpendicular to the cylinder axes.

For a pair of cylinders adhering to a membrane under lateral tension, the indirect interaction is repulsive if the cylinders adhere to the same membrane side, and attractive for two cylinders adhering at opposite membrane sides (see section 3). For a membrane in a harmonic potential, the interaction of the cylinders is always attractive (see section 4). The latter situation applies, in first approximation, to supported or bound membranes.

These results are intuitively plausible: The curvature $h''(x)$ around a single cylinder adhering to the top of a membrane under lateral tension is negative (see eq. (5) and Fig. 2). This means that the membrane is 'curved away' from a second cylinder approaching the membrane from the same side, but 'curved towards' a cylinder approaching the membrane from the opposite side. The negative curvature makes it more difficult for a cylinder to adhere at the same side close to the first cylinder, but facilitates the adhesion of a second cylinder at the opposite side. In contrast, the profile around a single cylinder adhering to a membrane in a harmonic potential is an exponentially damped, oscillating profile, with both negatively and positively curved segments (see eq. (25) and Fig. 5).

For a membrane under lateral tension, the profile around a single adhering cylinder with axis at $x = 0$ is proportional to $\exp(-\xi|x|)$ (see section 3.1). Here, $\xi = \sqrt{\sigma/\kappa}$ is the characteristic reciprocal length of a membrane with tension σ. The same profile is obtained around a single wedge-shaped inclusion in a tense membrane (see appendix B.1). Similar membrane profiles are also obtained for a membrane with two cylinders or two wedge-shaped inclusions. However, the contact region of the adsorbed cylinders depends on the distance L of the cylinders, whereas the angle α and width D of the wedge-shaped inclusions are constant. Therefore, the interaction energy as a function of the distance L is different for adsorbed cylinders and for wedge-shaped inclusions (see eqs. (13), (21), (70), and (80)). For the same reason the interaction energy of adhering spheres should be different from the interaction energy of conical inclusions.

The strength of the cylinder interactions can be estimated from the energetic prefactors. For a membrane under lateral tension, the prefactor $(\kappa + 2R^2U)^2/(4\sqrt{\sigma\kappa}R^2)$ of the interaction energies (13) and (21) can be written as $(\delta_o/R)^2\sqrt{\sigma\kappa}$, where δ_o is the contact point at large separations L (see eq. 8). For $(\delta_o/R) \lesssim 0.5$, the typical bending rigidity $\kappa = 10^{-19}$ J and membrane tensions up to 10^{-3} N/m, the prefactor can attain values of up to 0.5 k_BT per nanometer length of the cylinders, leading to large interaction energies for colloidal cylinders with lengths of several hundred nanometers. For a membrane in an external potential, the prefactor $(\kappa+2R^2U)^2/(2\eta\kappa R^2)$ of the interaction energies (40) and (48) can be written in the form $2(\delta_o/R)^2\eta\kappa$ with δ_o given by eq. (27). For $\delta_o/R = 0.5$, a typical length scale $1/\eta = 50$ nm of about 10 times the membrane thickness, and $\kappa = 10^{-19}$ J, this prefactor has the value 0.25 k_BT/nm. The binding energy for two cylinders adhering at the same side then is about -0.025 k_BT per nanometer length of the cylinders (see Fig. 6), leading, e.g., to a binding energy of 10 k_BT for colloidal cylinders with a length of 400 nm. These estimates for the static interactions of the colloidal membrane-adsorbed cylinders

are clearly larger than the loss of orientational free energy of order k_BT per cylinder, which is caused by the parallel alignment. The interactions therefore can lead to stable pairs or bundles of such cylinders. However, for a membrane dominated by lateral tension, these conformations are only stable if the cylinders are adsorbed alternately on opposite membrane sides.

Attractive interactions and aggregation of spherical particles adsorbed on vesicles has been experimentally observed by Koltover, Rädler, and Safinya [10]. The particles do not aggregate in solution. Therefore, the attractive interactions are probably indirect, i.e. mediated by the membrane. Since the particles have a radius of 0.9 μm, the interactions are most likely due to the rather long-ranged fluctuation-induced interactions, or interactions from perturbations of the equilibrium membrane shape as considered here. Interactions due to membrane thickness perturbations typically decay over a few nanometers, a length-scale comparable to the membrane thickness [20,21,22, 23,24,25] . The fluctuation-induced pair interactions are always attractive, but rather weak compared to thermal energies [11,12,13,14,15,16]. Depending on the induced deformation, the static interactions considered in this paper can be strong, see above. Exploring the latter as a possible explanation for the observations made by Koltover et al. requires an extension of the calculations presented here to beads and to nonplanar membranes or vesicles.

Acknowledgements

I would like to thank Wolfgang Helfrich and Martin Brinkmann for helpful discussions.

A Single cylinder adhering to a finite membrane under lateral tension

In this appendix, we consider a single cylinder adhering to a *finite* membrane under lateral tension. In the limit of infinite membrane size, we will obtain and thus corroborate the profile and energy derived in section 3.1.

As in section 3.1, the membrane segment in contact with the cylinder for $-\delta_o < x < \delta_o$ has the circular profile (4). The profile $h(x)$ of the nonadhering finite membrane segment for $\delta_o < x < \Lambda$ has the general form (3) for $x > 0$. For symmetry reasons, we have $h(-x) = h(x)$. The four parameters C_1 to C_4 in (3) can be determined from the four boundary conditions:

$$h(\delta_o) = h_o + \frac{\delta_o^2}{2R}\,, \quad h(\Lambda) = 0 \tag{50}$$

$$h'(\delta_o) = \frac{\delta_o}{R}\,, \quad h'(\Lambda) = 0 \tag{51}$$

$$\tag{52}$$

Here, we again assume $\delta_o \ll R$, and determine C_1 to C_4 to first order in δ_o and h_o. The second order in δ_o and h_o, the elastic energy of the two outer membrane segments is

$$G_o = \sigma\Big[C_2^2 L + C_3^2\xi(1-e^{-2\xi\Lambda}) + C_4^2\xi(e^{2\xi\Lambda}-1) + 2C_2C_3(e^{-\xi\Lambda}-1) + 2C_2C_4(e^{\xi\Lambda}-1)\Big] \tag{53}$$

For given h_o and δ_o, the analytical expressions for the four parameters C_1 to C_4 are rather lengthy and not shown here. However, if we minimize the total free energy $G = G_z + G_o$ with G_z as in eq. (6) with respect to h_o and δ_o, we get

$$C_1 = -\frac{(\kappa + 2R^2U)}{2\sigma R\cosh(\xi\Lambda)} \tag{54}$$

$$C_2 = 0 \tag{55}$$

$$C_3 = \frac{(\kappa + 2R^2U)(\tanh(\xi\Lambda)+1)}{4\sigma R} \tag{56}$$

$$C_4 = -\frac{(\kappa + 2R^2U)(\tanh(\xi\Lambda)-1)}{4\sigma R} \tag{57}$$

For $\Lambda \to \infty$, we obtain $C_1 \to 0$, $C_3 \to (\kappa + 2R^2U)/(2\sigma R)$, and $C_4 \exp(\xi x) \to 0$. In the limit of infinite membrane size, we thus recover the equilibrium shape $h(x) = (\kappa + 2R^2U)\exp(-\xi x)/(2\sigma R)$ from section 3.1.

B Wedge-shaped inclusions

B.1 Single inclusion

A wedge-shaped inclusion is characterized by its diameter D and angle α. If the center of the inclusion is located at $x = 0$, a single inclusion imposes the boundary condition

$$h'(\pm D/2) = \pm\alpha \tag{58}$$

For a membrane under lateral tension, the profile around a single inclusion is given by

$$h(x) = A + B\exp(-\xi|x|) \tag{59}$$

as in the case of a single adhering cylinder (see section 2.1). From the boundary condition (58), one obtains

$$B = -\alpha\exp(\xi D/2)/\xi \tag{60}$$

The coefficient A in (59) is arbitrary and defines the reference plane. The elastic energy of the membrane around the inclusion is given by

$$G = \alpha^2\sqrt{\sigma\kappa} \tag{61}$$

B.2 Two inclusions with equal orientation

We now consider two inclusions of diameter D with 'inner' edges located at $x = \pm L$, and 'outer' edges located at $x = \pm(L+D)$. In this section, the two inclusions have the

same orientation. At their edges, the inclusions impose the boundary conditions

$$h'(\pm L) = \pm(\beta - \alpha) \tag{62}$$
$$h'(\pm(L+D)) = \pm(\beta + \alpha) \tag{63}$$

on the membrane where β is the tilt angle of the inclusions. The membrane profile is symmetric with $h(-x) = h(x)$, and decays to zero for $x \to \infty$. The profile of the 'inner' membrane segment between the inclusions is given by

$$h(x) = C + D\cosh(\xi x) \tag{64}$$

From the boundary condition (62), one obtains

$$D = \frac{\beta - \alpha}{\xi \sinh(\xi L)} \tag{65}$$

The energy of the 'inner' membrane segment then is given by

$$G_\iota = (\beta - \alpha)^2 \sqrt{\sigma\kappa} \coth(\xi L) \tag{66}$$

The 'outer' membrane segments for $|x| > (L+D)$ have again the shape (60). The boundary condition (63) is fulfilled for

$$B = -(\beta + \alpha)\exp(\xi(L+D))/\xi \tag{67}$$

and the elastic energy of the two 'outer segments is

$$G_o = (\alpha + \beta)^2 \sqrt{\sigma\kappa} \tag{68}$$

As in the previous section, the coefficient A in (59) is arbitrary. Minimizing the total membrane energy $G = G_\iota + G_o$ with respect to the tilt angle β of the inclusions leads to the equilibrium value

$$\beta = \alpha \exp(-2\xi L) \tag{69}$$

and the interaction energy

$$\boxed{G(L) = 2\alpha^2 \sqrt{\sigma\kappa}(1 + \exp(-2\xi L))} \tag{70}$$

B.3 Two inclusions with opposite orientation

If the two inclusions have opposite orientation with respect to the membrane plane, the boundary conditions at the inclusion edges are

$$h'(\pm L) = (\beta - \alpha) \tag{71}$$
$$h'(\pm(L+D)) = (\beta + \alpha) \tag{72}$$

and

$$h(\pm L) = \pm h_o \tag{73}$$

where h_o is the deviation of the inclusions out of the reference plane, and β is again the tilt angle. We now have the symmetry $h(-x) = -h(x)$. The profile of the 'inner' membrane segment between the inclusions is given by

$$h(x) = Cx + D\sinh(\xi x) \tag{74}$$

From the boundary conditions above, we obtain

$$C = \frac{\xi h_o \cosh(\xi L) + (\alpha - \beta)\sinh(\xi L)}{\xi L \cosh(\xi L) - \sinh(\xi L)} \tag{75}$$
$$D = -\frac{h_o + (\alpha - \beta)L}{\xi L \cosh(\xi L) - \sinh(\xi L)} \tag{76}$$

The energy of the 'inner' membrane segment is

$$G_\iota = \frac{\sigma}{2}\left(2C^2 L + 4CD\sinh(\xi L) + D^2 \xi \sinh(2\xi L)\right) \tag{77}$$

with C and D as given above. As in the previous section, the two outer membrane segments have the energy (68).

Minimizing the total membrane energy $G = G_\iota + G_o$ with respect to the tilt angle β and deviation h_o of the inclusions leads to the equilibrium values

$$\beta = -\alpha \exp(-2\xi L) \tag{78}$$
$$h_o = -\alpha(1 - \exp(-2\xi L))/\xi \tag{79}$$

and the attractive interaction energy

$$\boxed{G(L) = 2\alpha^2 \sqrt{\sigma\kappa}(1 - \exp(-2\xi L))} \tag{80}$$

References

1. B. Alberts et al., *Molecular Biology of the Cell*, 3rd ed. (Garland, New York, 1994).
2. R. Lipowsky and E. Sackmann, *The Structure and Dynamics of Membranes* (Elsevier, Amsterdam, 1995).
3. K. Simons and E. Ikonen, Nature **387**, 569 (1997).
4. R. Schekman and L. Orci, Science **271**, 1526 (1996).
5. C.R.F. Monks, B.A. Freiberg, H. Kupfer, N. Sciaky, and A. Kupfer, Nature **395**, 82 (1998).
6. A. Grakoui, S.K. Bromley, C. Sumen, M.M. Davis, A.S. Shaw, P.M. Allen, and M.L. Dustin, Science **285**, 221 (1999).
7. S.L. Keller, W.H. Pitcher III, W.H. Huestis, H.M. McConnell, Phys. Rev. Lett. **81**, 5019 (1998).
8. C. Dietrich, L.A. Bagatolli, Z.N. Volovyk, N.L. Thompson, M. Leve, K. Jacobson, and E. Gratton, Biophys. J. **80**, 1417 (2001).
9. A. Albersdörfer, T. Feder, and E. Sackmann, Biophys. J. **73**, 245 (1997); A. Kloboucek, A. Behrisch, J. Faix, and E. Sackmann, Biophys. J. **77**, 2311 (1999); Z. Guttenberg, B. Lorz, E. Sackmann, and A. Boulbitch, Europhys. Lett. bf 54, 826 (2001).
10. I. Koltover, J.O. Rädler, and C.R. Safinya, Phys. Rev. Lett. **82**, 1991 (1999).
11. M. Goulian, R. Bruinsma, and P. Pincus, Europhys. Lett. **22**, 145 (1993); Erratum in Europhys. Lett. **23**, 155 (1993).
12. R.R. Netz and P. Pincus, Phys. Rev. E **52**, 4114 (1995); R.R. Netz, J. Phys. I France **7**, 833 (1997).
13. J.-M. Park and T.C. Lubensky, J. Phys. I France **6**, 1217 (1996).
14. R. Golestanian, M. Goulian, and M. Kardar, Europhys. Lett. **33**, 241 (1996); Phys. Rev. E. **54**, 6725 (1996).
15. P.G. Dommersnes and J.-B. Fournier, Europhys. Lett. **46**, 256 (1999); Eur. Phys. J. B **12**, 9 (1999)
16. W. Helfrich and T.R. Weikl, Eur. Phys. J. E **5**, 423 (2001).

17. T.R. Weikl, Europhys. Lett. **54**, 547 (2001); Phys. Rev. E. 66, 061915 (2002).
18. R. Bruinsma, M. Goulian, and P. Pincus, Biophys. J. **67**, 746 (1994).
19. T.R. Weikl, R.R. Netz, and R. Lipowsky, Phys. Rev. E **62**, R45 (2000); T.R. Weikl and R. Lipowsky, Phys. Rev. E **64**, 011903 (2001).
20. N. Dan, A. Berman, P. Pincus, and S. Safran, J. Phys. II France **4**, 1713 (1994).
21. J.-B. Fournier, Europhys. Lett. **43**, 725 (1998).
22. S. May and A. Ben-Shaul, Biophys. J. 76, 751 (1999).
23. T.A. Harroun, W.T. Heller, T.M. Weiss, L. Yang, and H.W. Huang, Biophys. J. **76**, 937 (1999).
24. P. Sens and S.A. Safran, Eur. Phys. J. E **1**, 237 (2000).
25. P. Schiller, Phys. Rev. E **62**, 918 (2000); Mol. Phys. **98**, 493 (2000).
26. T.R. Weikl, M.M. Kozlov, and W. Helfrich, Phys. Rev. E. **57**, 6988 (1998).
27. P.G. Dommersnes, J.-B. Fournier, and P. Galatola, Europhys. Lett. **42**, 233 (1998).
28. K.S. Kim, J. Neu, and G. Oster, Biophys. J. **75**, 2274 (1998); Europhys. Lett. **48**, 99 (1999).
29. T. Sintes, A. Baumgärtner, J. Phys. Chem. B **102**, 7050 (1998).
30. P.G. Dommersnes and J.-B. Fournier, Biophys. J. **83**, 2898 (2002).
31. M. Breidenich, R.R. Netz, and R. Lipowsky, Europhys. Lett. **49**, 431 (2000).
32. T. Bickel, C. Marques, and C. Jeppesen, Phys. Rev. E **62**, 1124 (2000); T. Bickel, C. Jeppesen, and C.M. Marques, Eur. Phys. J. E **4**, 33 (2001).
33. A. Boulbitch, Europhys. Lett. **59**, 910-915 (2002).